Supramolecular Architectures For Controlling Slow Magnetic Relaxation in Field-Induced Single-Molecule Magnets.

Fatemah Habib,[a] Jérôme Long,[a] Po-Heng Lin,[a] Ilia Korobkov,[a] Liviu Ungur,[c] Wolfgang Wernsdorfer,[d] Liviu F. Chibotaru,[c] Muralee Murugesu*[a,b]

[a] Department of Chemistry, University of Ottawa, 10 Marie Curie, Ottawa, ON, K1N6N5, Canada.
Tel: +1 613 562 5800-2733; E-mail: m.murugesu@uottawa.ca
[b] Centre for Catalysis Research and Innovation, 30 Marie-Curie, Ottawa, ON, K1N6N5, Canada.
[c] Division of Quantum and Physical Chemistry and INPAC—Institute for Nanoscale Physics and Chemistry, Katholieke Universiteit Leuven, Celestijnenlaan, 200F, 3001, Belgium.
[d] Institut Néel, CNRS & Université J. Fourier, BP 166, 25 Avenue des Martyrs, 38042, Grenoble, France.

Experimental Section

***N,N'*-Bis(3-methoxysalicylidene)benzene-1,4-diamine (H_2L^1), *N,N'*-Bis(3-methoxysalicylidene)biphenyl-4,4'-diamine (H_2L^2), *N,N'*-Bis(3-methoxysalicylidene)-4,4'-methylenedianiline (H_2L^3)**: To a solution of *o*-vanillin (0.02 mol, 2 equiv.) in 20 mL ethanol was added a solution of *p*-phenylenediamine for **H_2L^1**, 4,4'-biphenyldiamine for **H_2L^2** and 4,4'-methylenedianiline for **H_2L^3** (0.01 mol, 1 equiv.) in 20 mL ethanol. The orange solution was refluxed for one hour then filtered after cooling down to room temperature. The resulting orange powder was washed with diethyl ether and ethanol. (Yield = 92% (**H_2L^1**), 89% (**H_2L^2**) and 91% (**H_2L^3**)). Selected IR for **H_2L^1** (KBr, cm^{-1}): 3405 (br), 2914 (w), 1610 (s), 1470 (s), 1250 (s), 1200 (s), 1070 (m), 970 (s), 840 (s), 780 (m), 740 (s). ^{1}H NMR ($CDCl_3$, 400 MHz): δ 3.93 (s, 3H, OCH_3), 6.88 (t, 1H, 7.8 Hz, Ar), 6.99 (d d, 2H, 1.5 Hz, Ar), 7.35 (s, 2H, Ar), 8.65 (s, 1H, N=CH) ppm. NMR ^{13}C ($CDCl_3$, 400 MHz): δ 56.24 (OCH_3), 114.95 (Ar), 118.67 (Ar), 119.12 (Ar), 122.31 (Ar), 123.85 (Ar), 146.94 (Ar), 148.52 (Ar), 151.45 (Ar,) 162.37 (N=CH) ppm. Selected IR for **H_2L^2** (KBr, cm^{-1}): 3480 (br), 1620 (s), 1470 (s), 1390 (w), 1250 (s), 1210 (m), 1080 (w), 970 (m), 820 (m), 730 (m). ^{1}H NMR ($CDCl_3$, 400 MHz): δ 3.94 (s, 6H, OCH_3), 6.88 (t, J = 7.9 Hz, 2H, Ar), 7.00 (dd, J = 16.1, 1.6 Hz, 2H, Ar), 7.02 (dd, J = 15.9, 1.6 Hz, 2H, Ar), 7.38 (d, J = 8.5 Hz, 4H, Ar), 7.66 (d, J = 8.4 Hz, 4H, Ar), 8.69 (s, 2H, N=CH) ppm. ^{13}C NMR ($CDCl_3$, 100 MHz): δ 56.2 (OCH_3), 114.9 (Ar), 118.6 (Ar), 119.2 (Ar), 121.8 (Ar), 123.8 (Ar), 128.0 (Ar), 139.1 (Ar), 147.4 (Ar), 148.6 (Ar), 151.5 (Ar,) 162.4 (N=CH) ppm. Selected IR for **H_2L^3** (KBr, cm^{-1}): 3470 (br), 1610 (s), 1470 (m), 1380 (w), 1260 (m), 1210 (w), 970 (w), 790 (w), 730 (m). ^{1}H NMR ($CDCl_3$, 400 MHz): δ 3.92 (s, 6H, OCH_3), 4.02 (s, 2H, CH_2), 6.86 (t, J = 7.8 Hz, 2H, Ar), 6.97 (dd, J = 10.8, 1.5 Hz, 2H, Ar), 6.99 (dd, J = 10.4, 1.5 Hz, 2H, Ar), 7.19-7.26 (m, 8H, Ar), 8.61 (s, 2H, N=CH) ppm. ^{13}C NMR ($CDCl_3$, 100 MHz): δ 41.0 (CH_2), 56.2 (OCH_3), 114.7 (Ar), 118.5 (Ar), 119.2 (Ar), 122.4 (Ar), 123.7 (Ar), 129.9 (Ar), 139.9 (Ar), 146.4 (Ar), 148.5 (Ar), 151.5 (Ar,) 162.1 (N=CH) ppm.

$(NEt_4)_2[Dy_2(L^1)_4]((CH_3)_2CO)_{0.25}$ (1) and **$(NEt_4)_2[Dy_2(L^3)_4](Et_2O)_2((CH_3)_2CO)_{1.5}$ (3)**: A solution of $Dy(NO_3)_3{\cdot}6H_2O$ (0.057 g, 0.125 mmol) in DMF (5 mL) was added to an orange solution of H_2L^1 for **1** and H_2L^3 for **3** (0.250 mmol) and TEAOH (334 μL, 0.500 mmol, 25% in MeOH) in acetone (20 mL). The mixture was sonicated then filtered. The filtrate was left undisturbed and yellow needles were observed after three days in ~ 35% and 37% yield for **1** and **3**, respectively. Selected IR data for **1** (KBr pellets, cm^{-1}): 3420 (br), 2970 (w), 1710 (m), 1680 (m), 1590 (s), 1480 (s), 1430 (s), 1340 (m), 1220 (s), 1170 (s), 1070 (m), 970 (w), 850 (s), 740 (s). Selected IR data for **3** (KBr pellets, cm^{-1}): ν = 3460 (br), 1620 (s), 1440 (m), 1380 (m), 1230 (s), 1070 (w), 850 (m), 730 (w).
Crystal data for **1**: $C_{104.75}H_{113.5}Dy_2N_{10}O_{16.25}$, M = 2097.56, monoclinic, *P2₁/n*, a = 21.5894(8) Å, b = 20.9227(9) Å, c = 23.8146(9) Å, α = 90°, β =, 109.321(2)°, γ = 90°, V = 10151.4(7) Å^3, R_1 = 0.0466, wR_2 = 0.1296. Crystal data for **3**: $C_{144.5}H_{165}Dy_2N_{10}O_{19.5}$, M = 2678.87, monolinic, *P-2₁/n*, a = 11.7840(15) Å, b = 22.870(3) Å, c = 52.230(6) Å, α = 90°, β = 95.811(6)°, γ= 90°, V = 14003(3) Å^3, R_1 = 0.0763, wR_2 = 0.1893.

$(NEt_4)_2[Dy_2(L^2)_4](H_2O)(DMF)_{0.5}$ (2): Tetraethylammonium hydroxide (TEAOH) (334 μL, 0.5 mmol, 25% in MeOH) was added to a pale orange solution of H_2L^2 (0.112 g, 0.250 mmol) in DMF (20 mL). After complete dissolution was observed, $Dy(NO_3)_3{\cdot}6H_2O$ (0.057 g, 0.125 mmol) was added and the reaction mixture was sonicated for five minutes. The pale orange mixture was filtered and the filtrate was left undisturbed. Yellow needles were isolated the next day in ~ 55% yield. Selected IR data for **2** (KBr pellets, cm^{-1}): ν = 3480 (br), 1610 (s), 1590 (s), 1540 (w), 1480 (s), 1440 (s), 1380 (m), 1230 (s), 1180 (m), 1070 (w), 740 (m).
Crystal data for **2**: $C_{129.5}H_{133.5}Dy_2N_{10.5}O_{17.5}$, M = 2441.97, triclinic, *P-1*, a = 14.3544(8) Å, b = 18.9741(10) Å, c = 23.0490(12) Å, α= 86.019(3)°, β= 81.988(3)°, γ= 79.315(2)°, V = 6102.5(6) Å^3, R_1 = 0.0805, wR_2 = 0.1588. CCDC 785130 (**1**), 818518 (**2**)

and 818519 (**3**) contain the supplementary crystallographic data for this paper. This data can be obtained free of charge from The Cambridge Crystallographic Data Centre via www.ccdc.cam.ac.uk/ data_request/cif.

Magnetism:

The magnetic susceptibility measurements were obtained using a Quantum Design SQUID magnetometer MPMS-XL7 operating between 1.8 and 400 K for dc applied fields ranging from –7 to 7 T. Measurements were performed on ground polycrystalline samples. The magnetic data were corrected for the sample holder and the diamagnetic contribution. The samples were checked for the presence of ferromagnetic impurities, which were absent in all three samples, by measuring the magnetization as a function of the field at 100 K.

Other Studies:

Infrared spectra were recorded in the solid state (KBr pellets) on a Nicolet Nexus 550 FTIR spectrometer in the 700-4000 cm^{-1} range. Nuclear magnetic resonance analyses were conducted on a Bruker Avance 400 equipped with an automatic sample charger and a 5 mm auto-tuning broadband probe with Z gradient.

X-Ray Crystallography:

Crystals were grown from Acetone/DMF for **1** and **2** and DMF for **3**. Single yellow crystals suitable for X-ray diffraction measurements were mounted on a glass fibre. Unit cell measurements and intensity data collections were performed on a Bruker-AXS SMART 1 k CCD diffractometer using graphite monochromated Mo *K*α radiation ($\lambda = 0.71073$ Å). The data reduction included a correction for Lorentz and polarization effects, with an applied multi-scan absorption correction (SADABS).

The crystal structures were solved and refined using the SHELXTL program suite.[1] Direct methods yielded all non-hydrogen atoms which were refined with anisotropic thermal parameters. All hydrogen atom positions were calculated geometrically and were riding on their respective atoms.

Table S1. Selected bond distances (Å) for complexes **1**-**3**.

Complex 1			
Dy1-O1	2.214(6)	Dy2-O3	2.258(6)
Dy1-O5	2.269(5)	Dy2-O4	2.590(6)
Dy1-O6	2.585(6)	Dy2-O7	2.219(7)
Dy1-O9	2.211(6)	Dy2-O11	2.225(6)
Dy1-O13	2.228(6)	Dy2-O12	2.633(6)
Dy1-O14	2.622(6)	Dy2-O15	2.220(7)
Dy1-N1	2.658(7)	Dy2-N4	2.654(7)
Dy1-N5	2.678(7)	Dy4-N8	2.661(8)
Complex 2			
Dy1-O1	2.197(10)	Dy2-O3	2.246(10)
Dy1-O5	2.261(10)	Dy2-O4	2.667(10)

---

[1] (1) Sheldrick, G. M.; *Acta Cryst*. **2008**, *A64*, 112-122.

Dy1-O6	2.611(10)	Dy2-O7	2.214(10)
Dy1-O9	2.198(10)	Dy2-O11	2.254(10)
Dy1-O13	2.262(9)	Dy2-O12	2.565(9)
Dy1-O14	2.637(10)	Dy2-O15	2.227(10)
Dy1-N1	2.660(11)	Dy2-N4	2.625(13)
Dy1-N5	2.573(12)	Dy4-N8	2.619(12)
Complex 3			
Dy1-O1	2.259(6)	Dy2-O3	2.201(7)
Dy1-O2	2.558(7)	Dy2-O7	2.234(7)
Dy1-O5	2.223(7)	Dy2-O8	2.659(7)
Dy1-O9	2.258(7)	Dy2-O11	2.185(7)
Dy1-O10	2.547(7)	Dy2-O15	2.228(7)
Dy1-O13	2.205(8)	Dy2-O16	2.637(7)
Dy1-N3	2.639(9)	Dy2-N2	2.642(8)
Dy1-N7	2.628(9)	Dy4-N6	2.651(8)

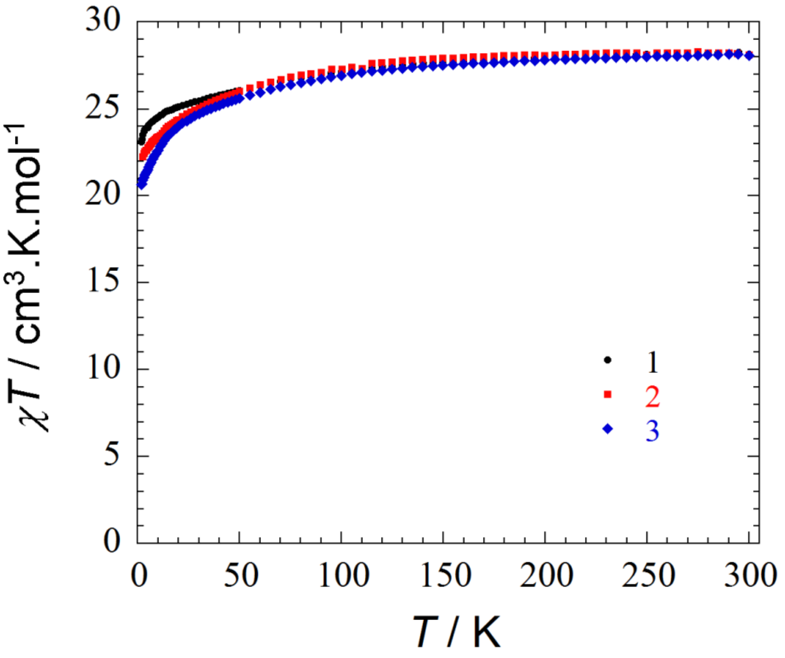

Figure S1. Plot of χT *vs.* T for complexes **1**, **2** and **3** in an applied dc field of 1000 Oe in the temperature range of 1.9-300 K.

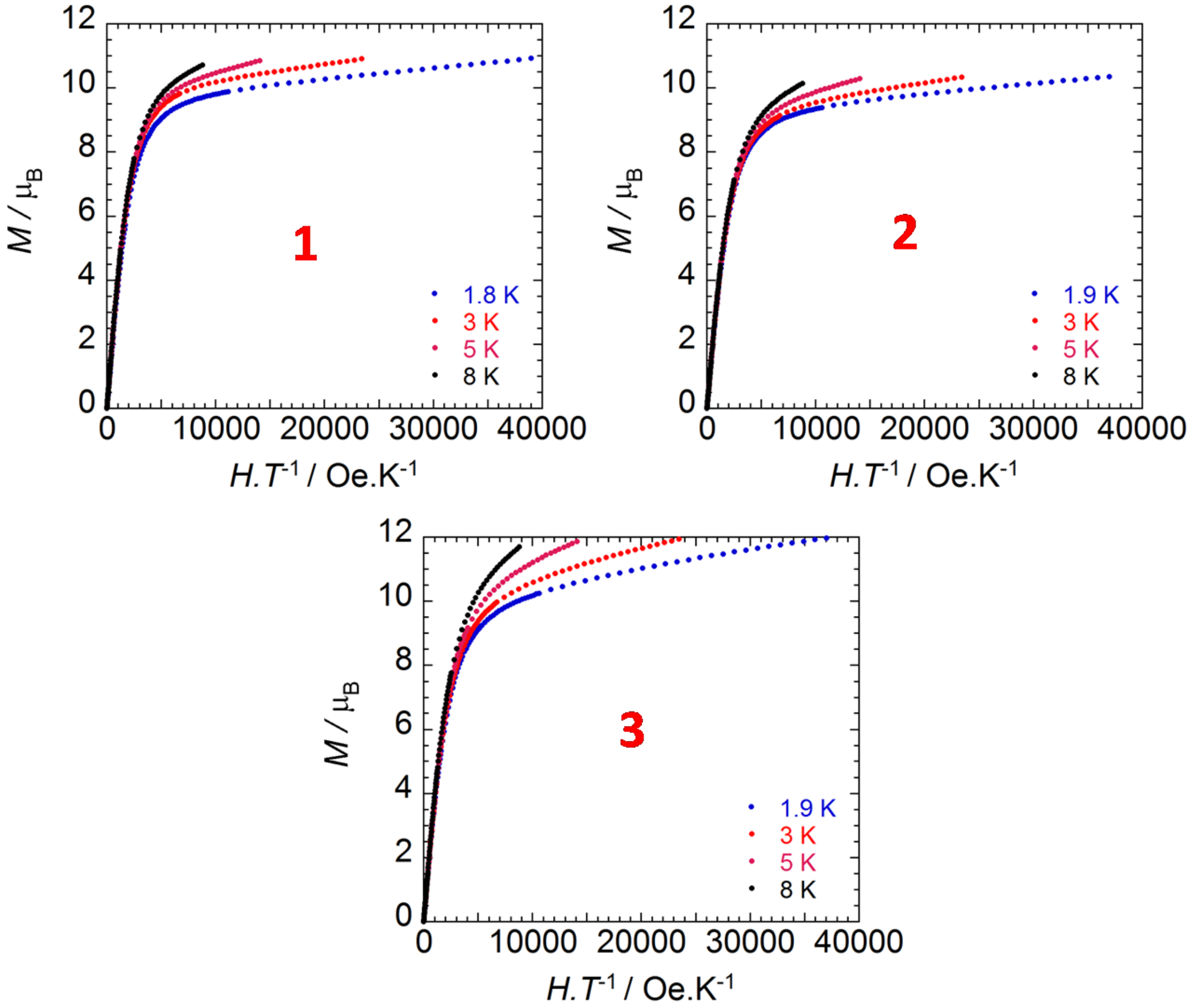

Figure S2: Reduced magnetization plots, *M vs. H/T*, for complexes **1-3**.

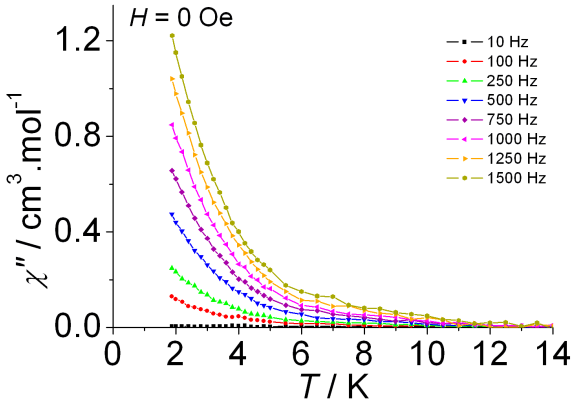

Figure S3: Frequency dependence of the out-of-phase (χ'') ac susceptibility from 1.8 to 14 K under zero dc field for **1**.

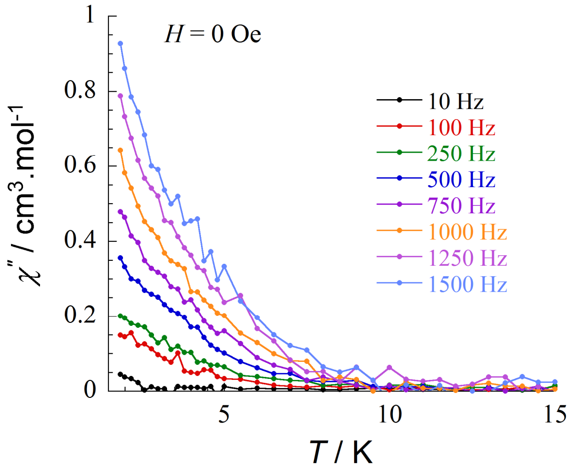

Figure S4: Frequency dependence of the out-of-phase (χ'') ac susceptibility from 1.8 to 15 K under zero dc field for **2**.

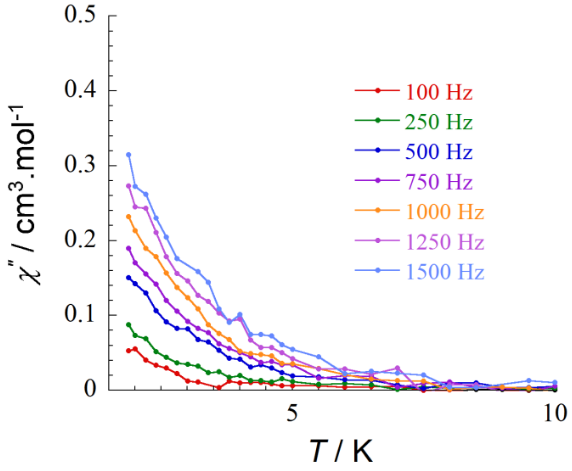

Figure S5: Frequency dependence of the out-of-phase (χ'') ac susceptibility from 1.8 to 10 K under zero dc field for **3**.

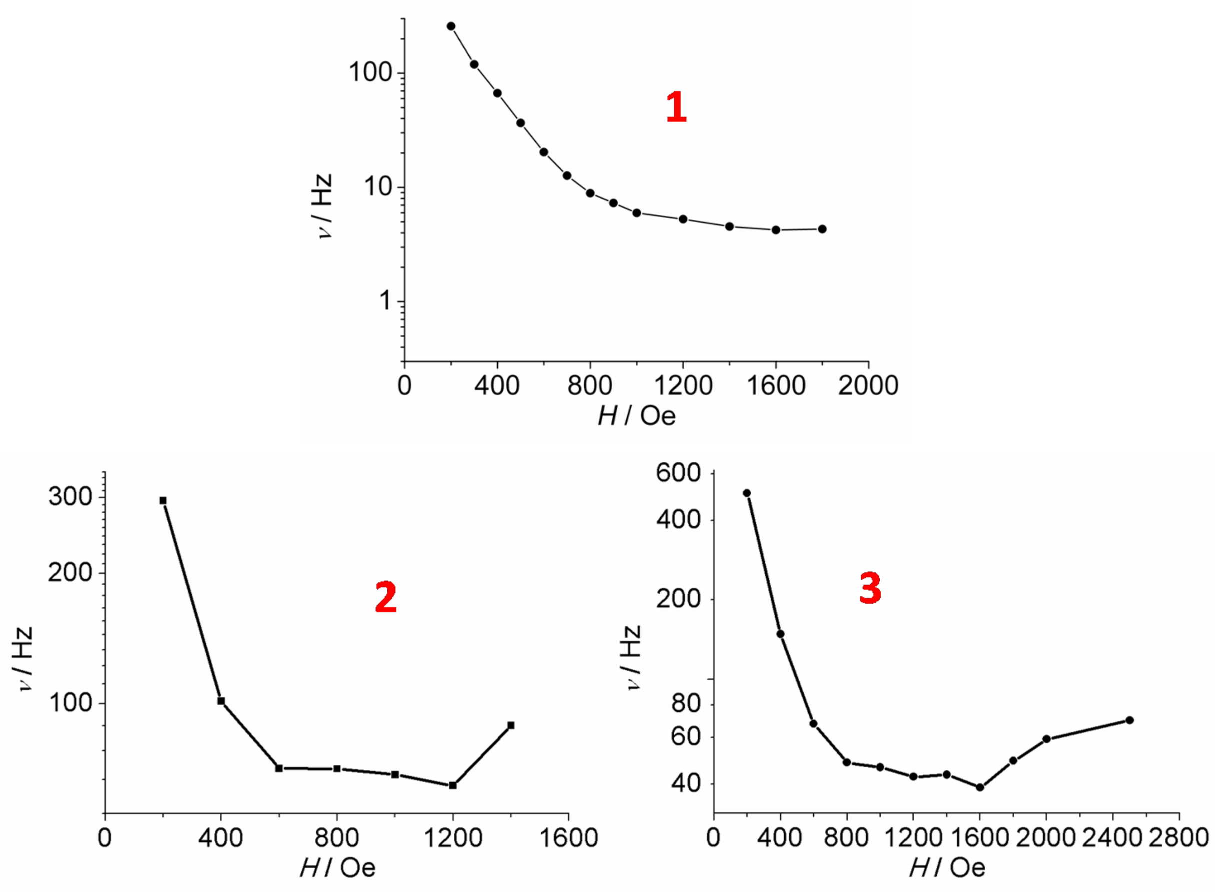

Figure S6: Field dependence of the characteristic frequency (maximum of χ'') as a function of the applied dc field for **1-3** at 2K. Line is guide for the eyes.

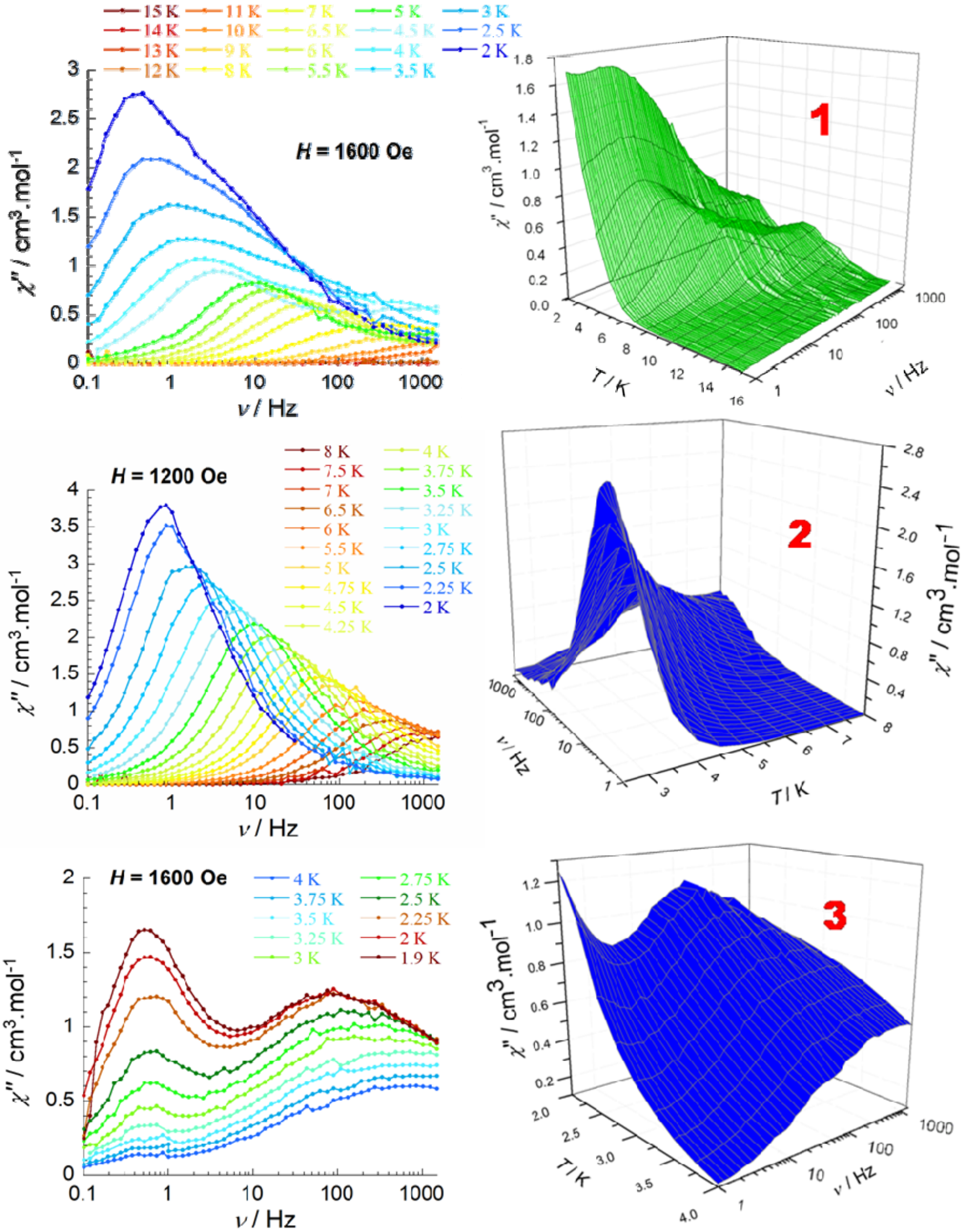

Figure S7: *Left*: Out-of-phase susceptibility χ'' *vs*. frequency ν (logarithmic scale) under applied dc fields of 1600 Oe for **1** and **3**, and 1200 Oe for **2**. *Right*: 3-D plots of χ'' *vs*. frequency ν (logarithmic scale) in the temperature ranges of 2-15 K (**1**), 2-8 K (**2**) and 2-4 K (**3**) under the same applied dc fields indicated on the left.

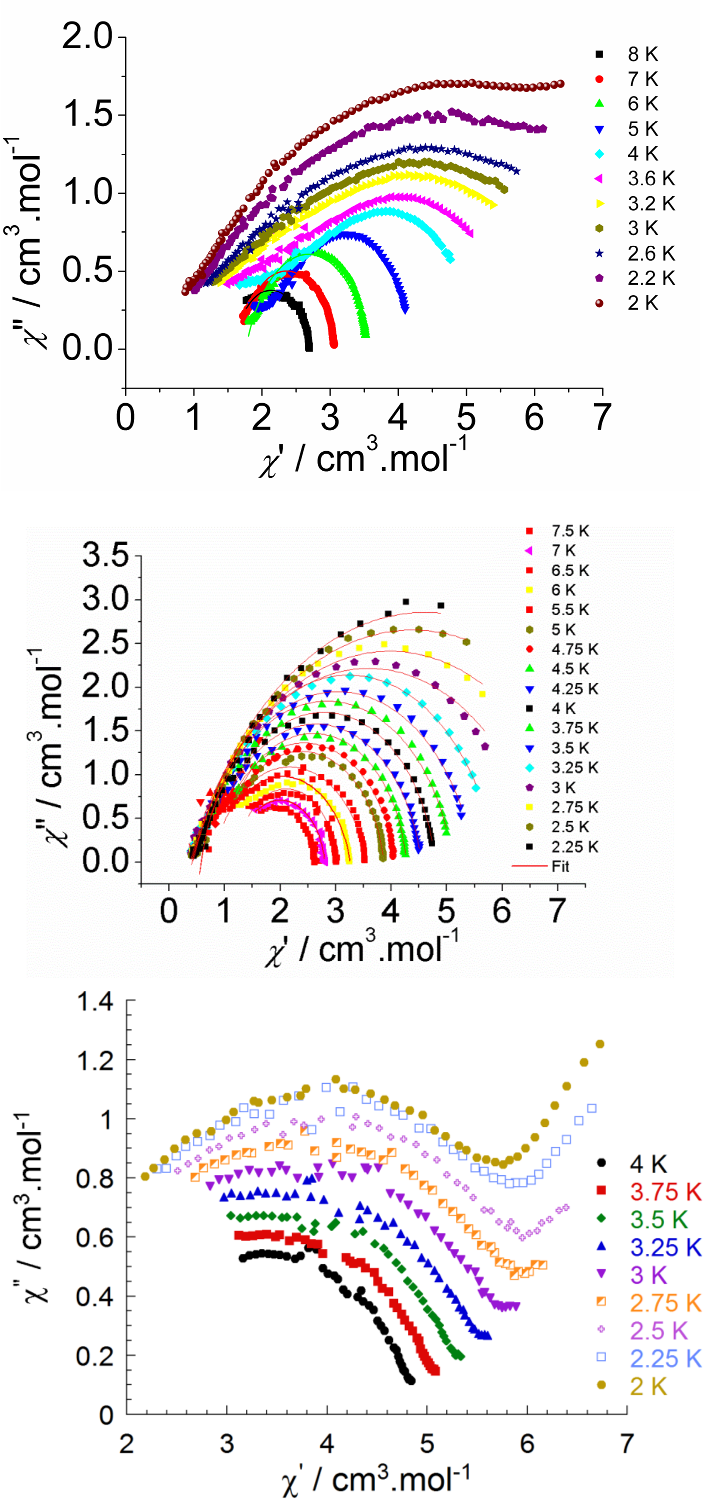

Figure S8: Cole-Cole (Argand) plots using the ac susceptibility data shown for **1** (*top*), **2** (*middle*) and **3** (*bottom*). The solid lines correspond to the best fits obtained with a generalized Debye model.

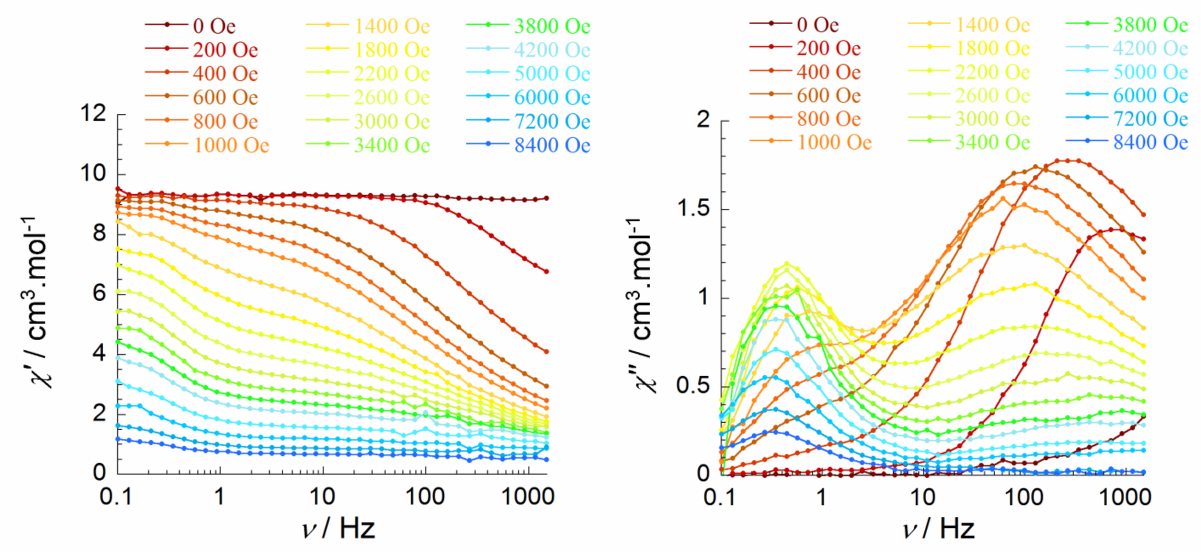

Figure S9: Plot of the real (left) and imaginary (right) *ac* susceptibilities *vs*. frequency (*ν*) measured at 1.9 K under applied dc fields ranging from 0- 8400 Oe for complex **3**.

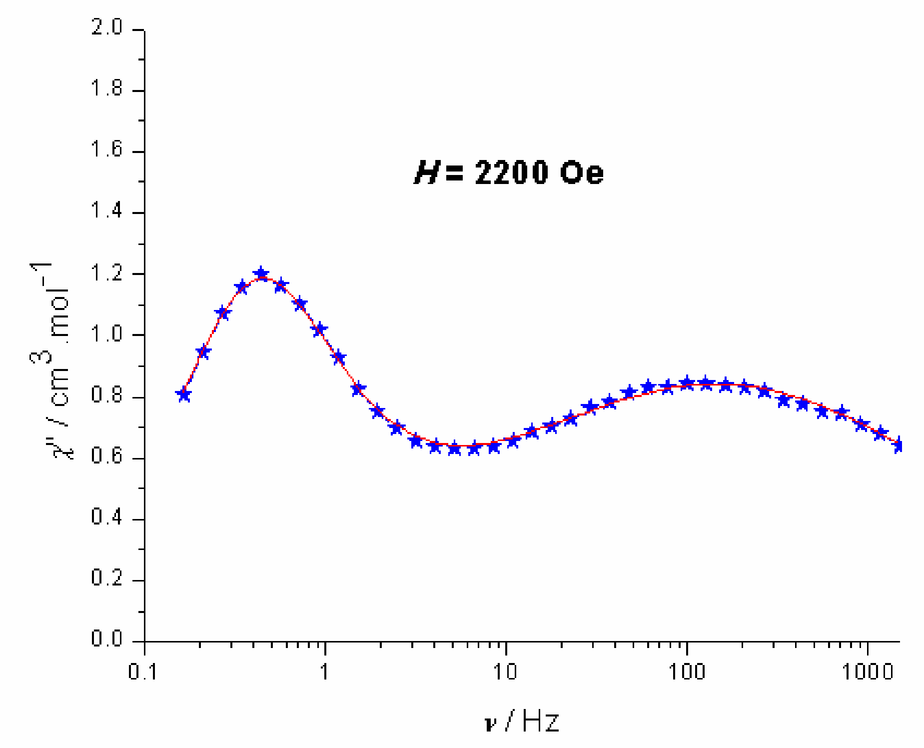

Figure S10: An example of the fitting of χ'' *vs*. frequency under an applied field of 2200 Oe using a convolution of two Casimir and Du Pré functions.[2]

---

(2) P.-E. Car, M. Perfetti, M. Mannini, A. Favre, A. Caneschi and R. Sessoli, *Chem Commun*., 2011, **47**, 3751 and references therein.

Best fit parameters obtained are: $(\chi_T - \chi_S)_{slow}$ = 1.96(1) emu/mol, τ_{slow} = 0.38(2) ms, α_{fast} = 0.36(4), $(\chi_T - \chi_S)_{fast}$ = 4.73(2) emu/mol, τ_{fast} = 9.68 x 10^{-4} ms, α_{fast} = 0.57(1), for the slow and fast relaxation processes.

Table S2: Extracted relaxation times for the slow and fast relaxation processes at 1.9 K and applied dc fields up to 8400 Oe for complex **3**.

Applied Field (Oe)	τ_{slow} (ms)	τ_{fast} (ms)
200	-	2.11E-04
300	-	3.42E-04
400	-	5.15E-04
500	-	7.22E-04
600	-	9.68E-04
700	-	9.68E-04
800	-	9.68E-04
900	-	9.68E-04
1000	0.21	9.68E-04
1200	0.17	9.68E-04
1400	0.19	9.68E-04
1600	0.28	9.68E-04
1800	0.34	9.68E-04
2000	0.36	9.68E-04
2200	0.38	9.68E-04
2400	0.41	9.68E-04
2600	0.40	9.68E-04
2800	0.41	9.68E-04
3000	0.40	9.68E-04
3200	0.39	9.68E-04
3400	0.44	9.68E-04
3600	0.41	9.68E-04
3800	0.43	-
4000	0.41	-
4200	0.39	-
4400	0.39	-
4600	0.42	-
4800	0.48	-
5000	0.41	-
6000	0.53	-
6400	0.52	-
6800	0.52	-
7200	0.50	-

7600	0.48	-
8000	0.51	-
8400	0.50	-
8800	0.49	-

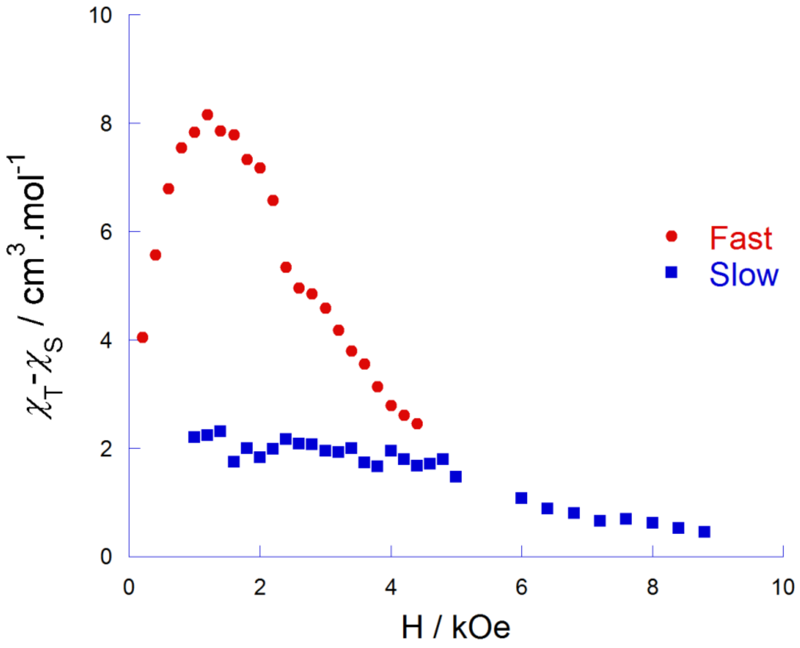

Figure S11: Plot of the difference between isothermal and adiabatic susceptibility (χ_T-χ_S) *vs*. H for the slow and fast relaxation processes derived from fitting of the χ'' *vs*. frequency curves for complex **3**.

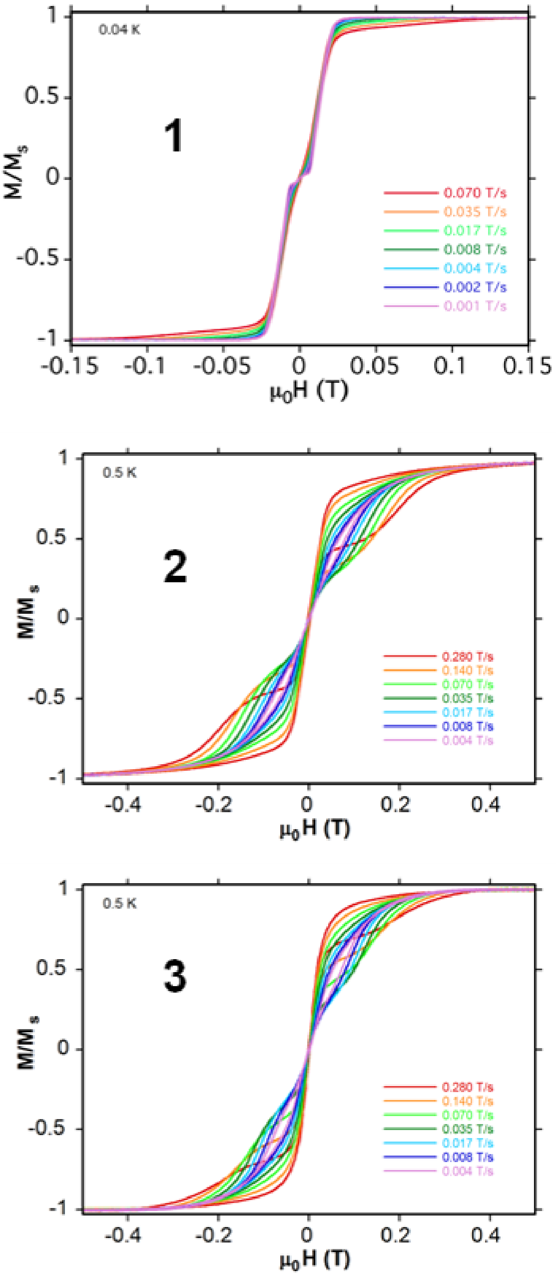

Figure S12: Magnetization (*M*) vs. applied dc field sweeps at the indicated sweep rates and temperature. *M* is normalized to its saturation value, *Ms*, at 0.3 T for **1** (*top*), **2** (*middle*) and **3** (*bottom*).

Ab initio calculations of electronic and magnetic properties of compounds 1, 2 and 3.

Computational details

All calculations were done with MOLCAS 7.6. All basis sets were taken from the ANO-RCC basis et library available from MOLCAS.

The calculations were done on mononuclear Dy centers which were obtained from "cutting" a sufficiently large fragment from the initial complex, with subsequent saturation of all broken bonds by hydrogens.

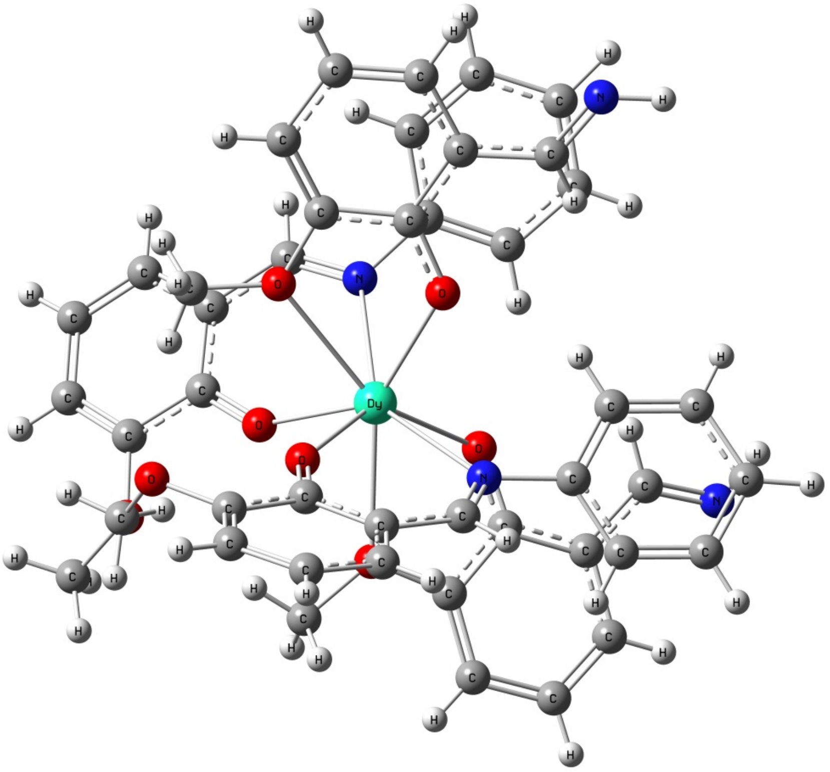

Figure S13. The structure of the calculated fragment of the center Dy1 of the compound **1**. Similar structures have been obtained from "cutting" other mononuclear Dy centers.

Results of the ab initio calculations:

Table S3. Energies of the spin-free states (cm^{-1}) for all calculated Dy centers.

2S+1		1		2		3	
		Dy1	**Dy2**	**Dy1**	**Dy2**	**Dy1**	**Dy2**
6	H	0.000	0.000	0.000	0.000	0.000	0.000
		6.600	5.741	25.403	20.478	20.033	8.015
		110.579	89.574	93.528	89.539	88.857	68.232
		161.588	131.498	195.392	170.542	144.927	92.511
		308.856	296.619	231.468	236.028	253.450	256.037
		319.788	308.460	248.658	257.038	263.958	272.588
		349.958	327.380	289.632	290.377	354.952	390.187
		433.523	432.560	524.032	500.801	544.983	536.689
		470.974	467.489	526.429	524.107	579.440	583.326
		627.826	633.175	577.610	609.950	628.532	689.953
		632.778	635.829	590.505	621.589	630.541	696.733
	F	7581.462	7581.625	7551.107	7557.784	7595.551	7618.732
		7702.766	7688.389	7702.555	7700.922	7690.231	7677.715
		7708.147	7695.959	7732.217	7727.014	7728.721	7717.418
		7812.956	7796.384	7777.540	7780.444	7790.072	7801.644
		7833.572	7821.128	7793.167	7797.232	7817.534	7826.667
		7862.188	7863.343	7865.962	7869.340	7903.474	7922.280
		7871.371	7865.857	7874.680	7880.359	7907.951	7925.723
	P	34838.010	34811.870	34793.347	34774.584	34730.611	34689.630
		34986.309	34973.581	35083.027	35064.535	35106.756	35076.765
		35355.865	35369.310	35258.313	35305.336	35357.896	35442.284
4		24900.492	24902.905	24892.222	24898.095	24909.809	24907.224
		24904.185	24906.959	24905.672	24900.026	24913.062	24912.452
		24937.765	24928.346	24908.672	24910.996	24931.604	24928.200
		24948.500	24930.940	24909.973	24922.347	24933.447	24932.029
		24972.070	24965.972	24924.206	24929.923	24967.353	24981.159
		24996.593	24995.813	24964.707	24961.859	24996.492	25004.885
		25007.233	25001.237	24969.242	24970.553	25011.949	25026.111
		25017.211	25014.860	24975.876	24987.891	25023.970	25040.617
		25113.488	25105.564	25078.275	25080.929	25113.558	25116.039
		25121.437	25109.018	25096.311	25097.454	25120.463	25133.129
		25128.201	25113.270	25109.793	25100.919	25145.576	25164.214
		25161.175	25161.226	25121.312	25129.447	25168.810	25200.030
		25215.506	25207.173	25212.671	25215.191	25232.441	25233.564
		25268.659	25254.501	25250.817	25251.422	25260.333	25260.975
		25298.565	25293.202	25277.482	25280.523	25309.207	25305.457
		25308.937	25300.187	25290.035	25294.743	25318.261	25322.547
		25319.816	25321.451	25302.359	25302.656	25334.023	25329.915
		25338.437	25327.052	25320.216	25315.018	25342.859	25352.894
		25347.677	25337.326	25333.128	25329.008	25352.248	25359.464
		25366.128	25361.373	25347.923	25353.114	25375.250	25374.648
		25382.993	25370.397	25369.334	25379.451	25383.200	25385.309
		25391.185	25381.461	25375.697	25386.472	25391.788	25401.475
		25394.116	25389.471	25390.755	25388.331	25398.029	25406.895
		25396.758	25391.995	25397.316	25404.249	25401.171	25409.766
		25417.853	25406.299	25420.574	25416.438	25413.620	25416.071

		25467.683	25454.414	25455.689	25454.604	25460.276	25450.443
		25476.770	25463.878	25463.770	25469.023	25489.931	25465.996
		25487.733	25476.870	25509.007	25500.234	25493.536	25501.787
		25515.548	25504.618	25527.118	25526.463	25523.232	25511.698
		...	...	...	...	...	...
2		37372.556	37372.794	37349.538	37356.007	37374.117	37380.876
		37376.323	37376.781	37355.516	37358.601	37378.445	37386.062
		37390.560	37386.290	37358.798	37366.551	37384.672	37387.110
		37394.017	37389.910	37365.325	37369.292	37390.362	37393.358
		37406.671	37409.314	37378.916	37387.179	37420.131	37437.075
		37412.735	37414.598	37384.311	37391.305	37425.510	37440.045
		37431.233	37432.583	37401.075	37409.718	37442.597	37455.674
		37440.391	37440.787	37407.815	37411.223	37451.327	37466.885
		37568.184	37559.914	37560.300	37561.207	37573.064	37573.063
		37586.239	37578.656	37587.775	37590.786	37592.847	37584.431
		37597.105	37589.480	37593.642	37595.840	37595.540	37594.633
		37607.398	37601.940	37614.305	37611.071	37622.456	37620.860
		37630.977	37625.076	37625.397	37621.601	37643.947	37643.503
		37636.948	37625.873	37631.746	37628.647	37646.453	37648.732
		37641.036	37634.515	37634.109	37634.103	37651.966	37651.724
		37664.201	37659.034	37659.685	37666.534	37667.222	37668.389
		37669.965	37661.930	37664.417	37668.643	37669.408	37672.287
		39038.015	39041.656	39028.933	39037.071	39046.581	39044.851
		39041.021	39046.151	39031.648	39041.195	39047.700	39049.408
		39062.260	39056.564	39044.452	39053.541	39058.873	39052.989
		39068.030	39063.242	39053.520	39063.212	39062.705	39058.725
		39110.656	39110.535	39083.580	39091.264	39123.583	39132.487
		39118.470	39117.226	39092.059	39096.870	39128.005	39135.825
		39128.303	39126.892	39108.104	39108.922	39144.393	39153.372
		39136.959	39133.671	39114.494	39114.395	39147.286	39158.423
		39256.695	39247.350	39250.696	39251.469	39270.149	39262.898
		39259.990	39256.873	39256.232	39255.375	39273.822	39268.974
		39278.047	39265.911	39268.738	39265.279	39276.107	39275.972
		39280.611	39267.097	39279.221	39275.490	39277.182	39285.694
		39301.312	39295.273	39303.083	39301.398	39320.109	39320.721
		39337.280	39331.549	39325.610	39335.062	39332.217	39342.892
		39343.838	39338.657	39335.781	39342.887	39345.272	39352.692
		...	...	...	...	...	...

Table S4. Energies of the lowest spin-orbit states (cm^{-1}) for all calculated Dy centers.

1		**2**		**3**	
Dy1	**Dy2**	**Dy1**	**Dy2**	**Dy1**	**Dy2**
0.000	0.000	0.000	0.000	0.000	0.000
84.673	35.949	32.006	33.178	35.213	23.186
188.389	174.765	128.350	149.267	150.660	151.513
261.400	224.617	172.365	162.891	188.216	204.627
280.272	255.672	217.691	231.915	284.406	315.618
339.640	333.953	295.743	318.143	378.089	420.868
381.069	373.018	409.286	395.247	461.115	486.755
575.630	570.385	475.851	523.651	553.629	634.138
3642.847	3630.571	3608.740	3604.802	3595.877	3589.860

3702.004	3658.629	3632.178	3637.657	3644.352	3643.717
3717.920	3696.815	3678.381	3682.604	3711.906	3724.106
3754.821	3733.890	3726.400	3733.985	3773.276	3791.433
3808.291	3794.210	3789.338	3795.934	3839.974	3860.256
3891.647	3883.793	3840.116	3857.138	3905.681	3948.913
4010.113	4004.482	3920.316	3956.439	4000.469	4071.353
6196.392	6161.245	6124.482	6123.069	6124.056	6123.002
6244.702	6238.753	6230.573	6237.492	6254.472	6260.781
6289.644	6264.402	6266.415	6265.301	6305.380	6312.363
6331.776	6307.845	6294.902	6299.492	6333.378	6352.734
6405.088	6393.509	6347.372	6369.399	6405.053	6442.763
6488.999	6483.060	6404.235	6435.397	6482.847	6548.153
8147.555	8115.917	8076.914	8078.359	8087.425	8091.115
8196.879	8186.873	8195.626	8199.758	8243.553	8249.855
8279.727	8255.805	8233.822	8236.620	8258.036	8273.951
8331.319	8315.109	8280.727	8297.651	8327.391	8357.167
8409.175	8402.135	8332.668	8360.295	8404.259	8462.328
9690.777	9661.660	9618.960	9621.682	9637.206	9642.940
9737.681	9723.924	9734.347	9733.917	9775.380	9785.731
9850.833	9831.515	9794.584	9810.021	9835.536	9860.560
9938.227	9930.734	9864.833	9890.075	9933.630	9988.418
10081.550	10064.631	10034.942	10047.297	10075.746	10089.262
10100.162	10082.417	10052.585	10063.753	10093.996	10104.545
10115.814	10093.438	10077.304	10083.868	10098.244	10121.645
10133.997	10119.317	10096.226	10104.170	10136.379	10164.347
10224.868	10199.539	10148.683	10164.229	10182.937	10209.369
10264.383	10254.006	10236.897	10251.065	10292.320	10324.683
10894.307	10865.391	10840.794	10838.243	10842.916	10840.809
10966.573	10949.441	10942.429	10951.397	10994.072	11014.701
11179.263	11173.429	11102.976	11129.558	11185.098	11248.235
11590.178	11569.787	11551.233	11555.860	11584.745	11598.970
11622.986	11602.913	11561.802	11576.638	11596.701	11619.868
11645.844	11627.010	11604.826	11614.058	11638.251	11659.587
11670.004	11657.586	11629.483	11644.739	11677.935	11705.117
11688.535	11669.656	11643.563	11655.731	11686.131	11713.140
13484.232	13468.384	13429.638	13442.135	13477.087	13504.352
13538.127	13520.489	13496.152	13509.060	13527.402	13546.803
13570.075	13552.012	13524.351	13535.218	13567.385	13591.084
13592.121	13572.105	13545.096	13553.719	13584.877	13608.508
14964.261	14947.661	14915.783	14929.822	14954.827	14977.876
14982.388	14965.471	14933.585	14944.251	14978.429	15003.529
15039.962	15020.288	14993.042	15002.554	15032.076	15055.171
15905.484	15886.786	15860.615	15870.356	15899.308	15920.346
15927.998	15910.627	15876.585	15889.001	15919.596	15945.836
16419.950	16402.864	16371.216	16383.421	16414.891	16440.836
…	…	…	…	…	…

Table S5. *g* tensors of the lowest doublet states for all calculated Dy centers.

		1		**2**		**3**	
		Dy1	**Dy2**	**Dy1**	**Dy2**	**Dy1**	**Dy2**
1	g_X	0.0312	0.0873	0.0701	0.1874	0.1342	0.0835
	g_Y	0.0403	0.2060	0.1462	0.3934	0.3842	0.4177
	g_Z	19.6312	18.8964	18.1150	17.6409	17.4299	15.9935
2	g_X	0.1091	0.0770	0.0310	0.1528	0.1794	0.1216
	g_Y	0.1907	0.1779	0.1999	0.3374	0.2628	0.3069
	g_Z	19.0868	18.2213	16.6259	16.1672	16.1418	15.1580
3	g_X	1.5558	1.4502	1.1476	0.8549	0.1978	0.1514
	g_Y	2.1101	1.4964	1.5376	2.0485	0.3147	0.1911
	g_Z	13.6421	13.2875	13.2694	12.7069	18.0342	18.3705
4	g_X	5.1587	0.2501	0.0420	0.1112	0.6909	0.6796
	g_Y	6.2693	0.3019	0.3594	0.6490	1.1424	1.1147
	g_Z	6.9611	18.8722	18.4598	18.2266	13.9055	12.4585
5	g_X	0.8160	3.3806	5.5506	6.0563	4.2256	3.1955
	g_Y	0.9260	6.4683	7.0940	6.8095	6.1961	4.7692
	g_Z	18.2414	7.7167	7.9502	8.1324	8.0513	8.4417
6	g_X	1.4260	1.0944	1.4872	1.1925	2.4945	1.5380
	g_Y	2.4854	3.7629	1.7392	1.2440	3.3070	4.6784
	g_Z	12.9775	12.0391	15.1287	15.6391	13.2319	8.4550
7	g_X	0.6610	1.2144	0.2245	0.0862	0.7426	1.5761
	g_Y	1.6538	3.6525	0.3099	0.1216	1.1488	4.1368
	g_Z	15.9456	15.0814	19.1706	19.2090	18.2303	15.0423
8	g_X	0.0062	0.0043	0.0294	0.0069	0.0351	0.0361
	g_Y	0.0113	0.0062	0.1184	0.0296	0.0645	0.0655
	g_Z	19.8191	19.8221	19.6029	19.7473	19.7242	19.7384

Table S6. Energies (cm^{-1}) of lowest exchange multiplets in **1-3** calculated in the presence of dipolar interaction.

Doublet	1	2	3
1	0.0	0.0	0.0
	0.0000012	0.000094	0.000033
2	0.072786836	0.001209796	0.001395540
	0.072789323	0.001306096	0.001436997
3	35.969243943	31.997809598	23.185653104
	35.969247545	31.997813093	23.185676953
4	36.001560539	32.015461503	35.215582161
	36.001562837	32.015466885	35.215626031
5	84.697267006	33.169975742	23.187760032
	84.697284673	33.169980687	23.187771935
6	84.721500781	33.187362845	35.213815261
	84.721523949	33.187364872	35.213863724

Calculation of the magnetic properties:

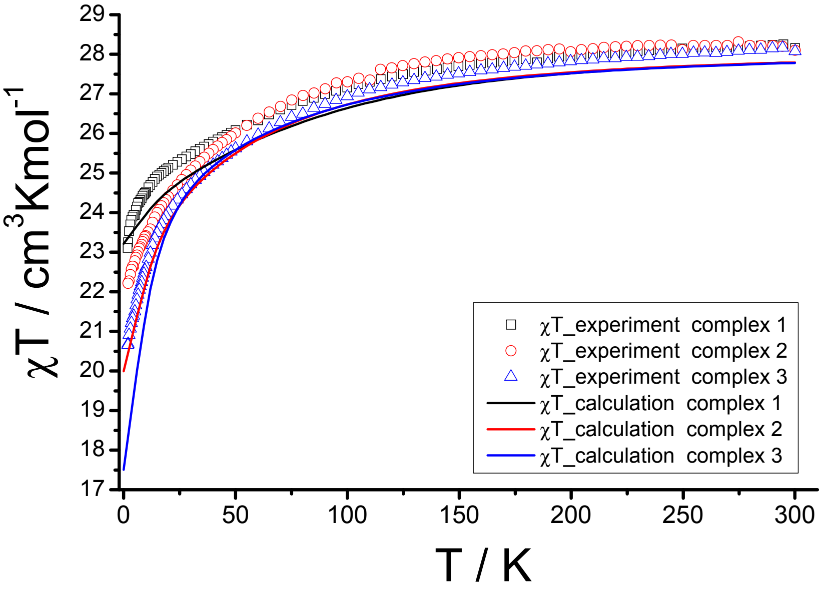

Figure S14. Comparison of the measured and calculated magnetic susceptibility for compounds **1**, **2** and **3**.

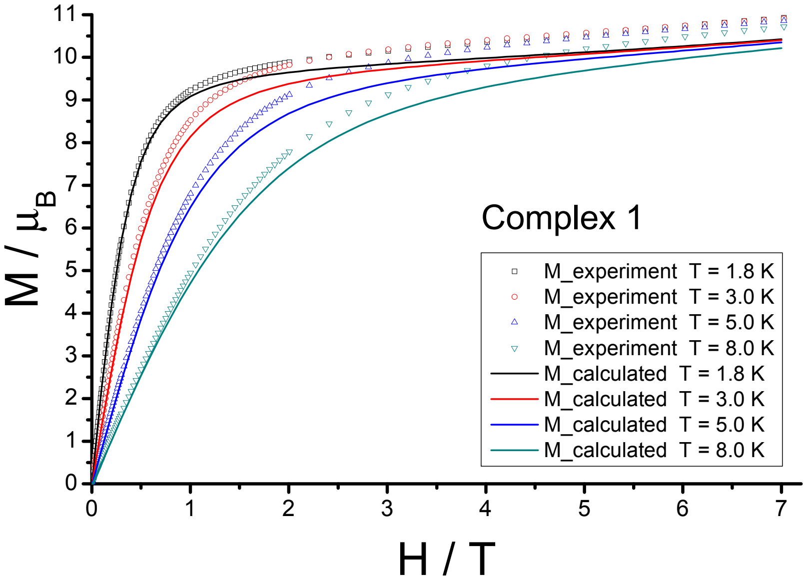

Figure S15. Comparison of the measured and calculated molar magnetization at low temperature for compound **1**.

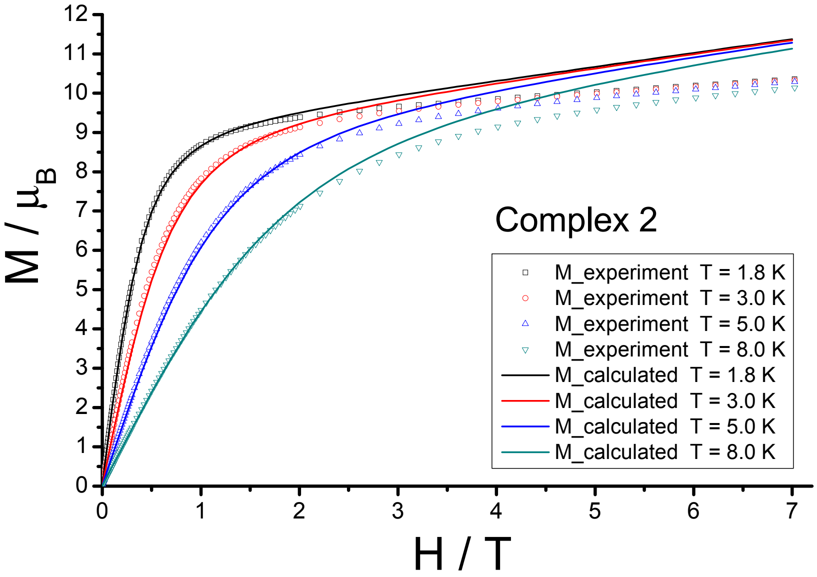

Figure S16. Comparison of the measured and calculated molar magnetization at low temperature for compound **2**.

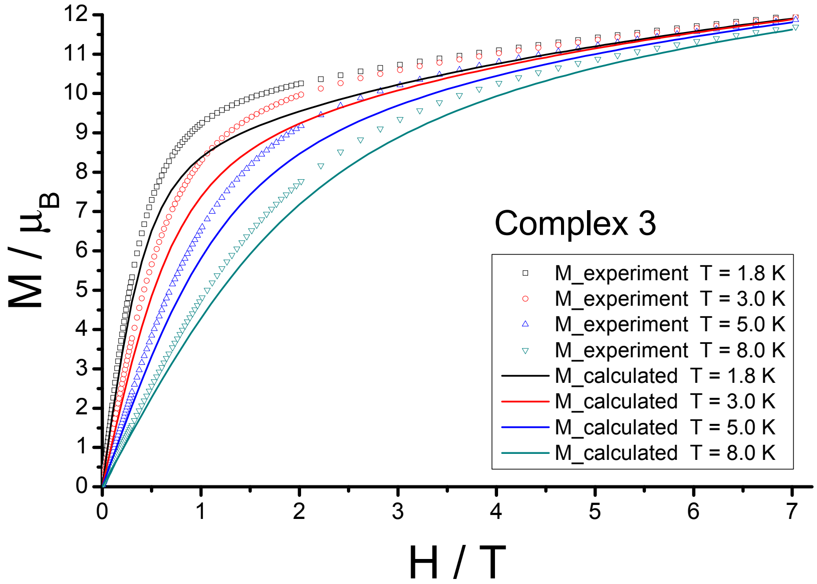

Figure S17. Comparison of the measured and calculated molar magnetization at low temperature for compound **3**.

Calculation of the magnetic properties with rescaled energy of the first excited Kramers doublet on Dy centers:

Table S7. Shift ($E_{rescaled}$-$E_{initial}$) of the energy of the first excited Kramers doublet (cm^{-1}) on Dy sites used for the calculation of the magnetic properties presented below. All other energies and all wave functions were not changed (see Table S3).

1		**2**		**3**	
Dy1	**Dy2**	**Dy1**	**Dy2**	**Dy1**	**Dy2**
-12.7	-7.2	+12.8	+13.3	+14.1	+9.3

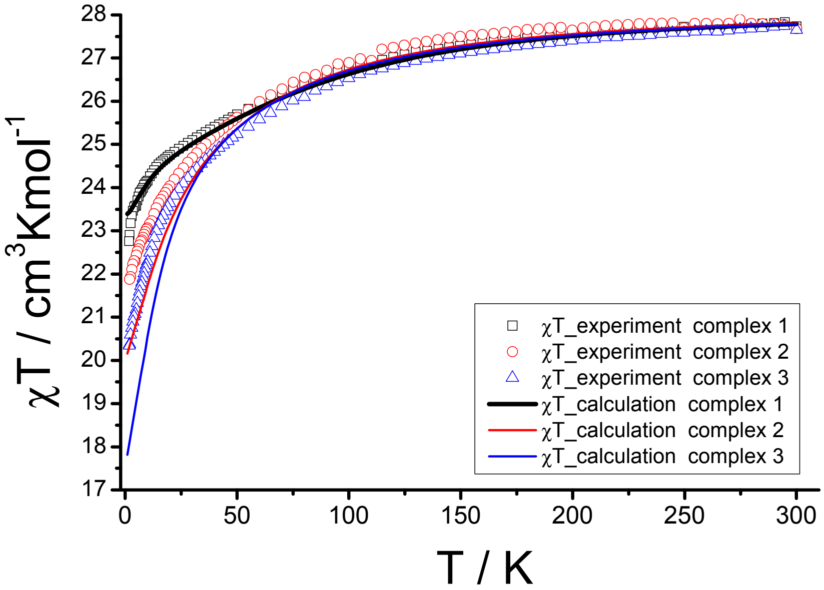

Figure S18. Comparison of the measured (downscaled by 1.5%) and calculated (with rescaled energy of the first excited KD on Dy centers) magnetic susceptibility for compounds **1**, **2** and **3**.

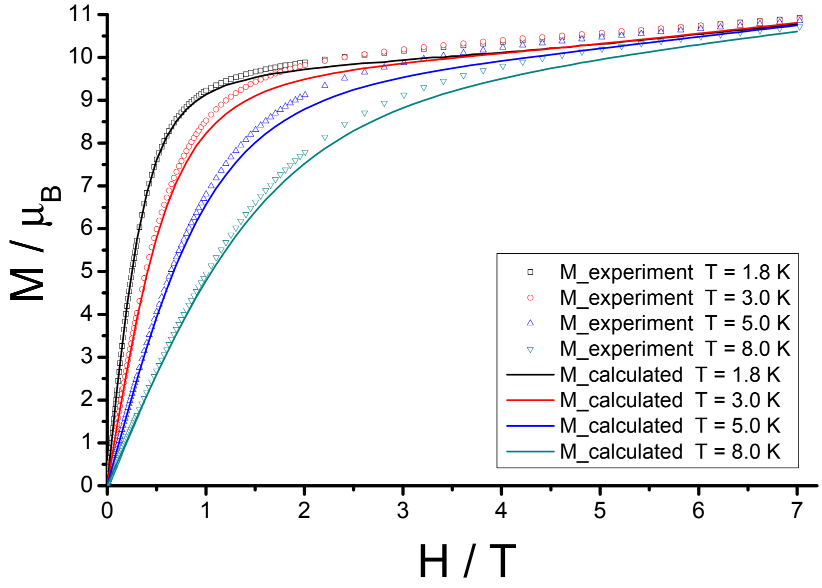

Figure S19. Comparison of the measured and calculated (with rescaled energy of the first excited KD on Dy centers) molar magnetization at low temperature for compound **1**.

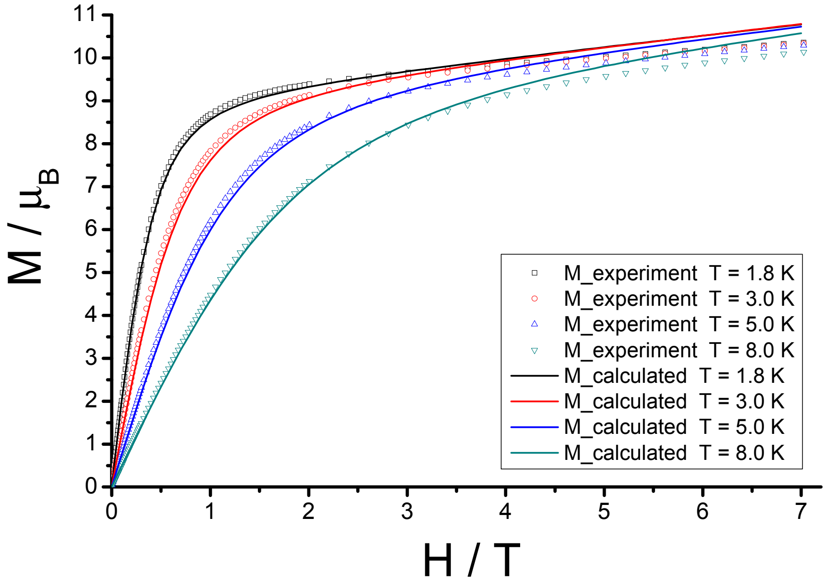

Figure S20. Comparison of the measured and calculated (with rescaled energy of the first excited KD on Dy centers) molar magnetization at low temperature for compound **2**.

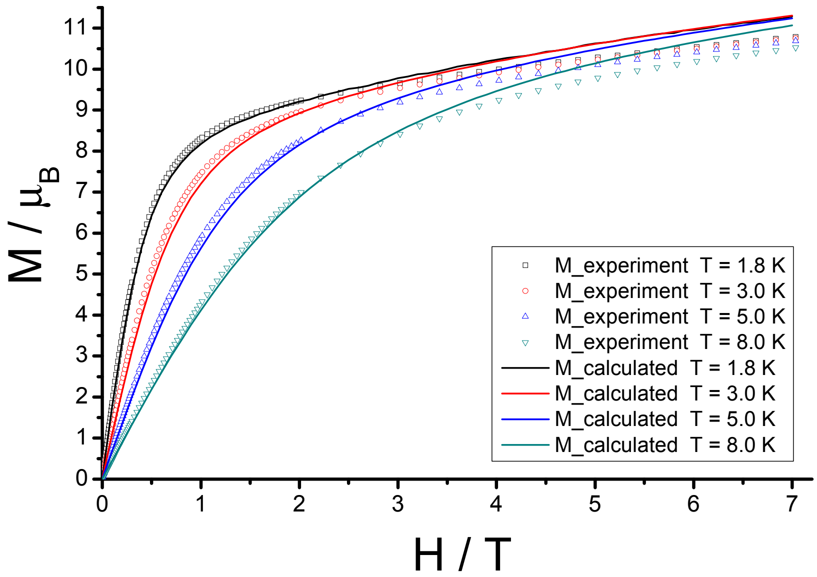

Figure S21. Comparison of the downscaled by 10% experimental molar magnetization and calculated (with rescaled energy of the first excited KD on Dy centers) molar magnetization at low temperature for compound **3**.